Asian Journal of Scientific Research

ISSN 1992-1454

science alert
http://www.scialert.net

ANSInet
an open access publisher
http://ansinet.com

Asian Journal of Scientific Research 4 (3): 224-235, 2011
ISSN 1992-1454 / DOI: 10.3923/ajsr.2011.224.235

Performance Prediction Procedures of the Supersonic Spiked Intakes

[1]Hussain H. Al-Kayiem, [2]Tawfiq W. Salih and [3]Abbas S.A. Al-Ambari
[1]Department of Mechnical Engeering, Universiti Teknologi PETRONAS, 31750, Tronoh, Perak, Malaysia
[2]Department of Mechnical Engeering, Al-Mustansirya University, Baghdad, Iraq
[3]Department of Mechnical Engeering, Wasit University, Wasit, Iraq

Corresponding Author: Hussain H. Al-Kayiem, Department of Mechnical Engeering, Universiti Teknologi PETRONAS, 31750, Tronoh, Perak, Malaysia

ABSTRACT

The supersonic flow approaching the intake of a supersonic aero engine must be brought to subsonic state before reaching the compressor face stage. The velocity reduction is combined with reduction in the total pressure of the flow which is not preferred by the designer of the supersonic gas turbine. In the present paper, analytical and two different numerical techniques were coupled to analyze the flow field in 2-D, compressible, supersonic spiked intake. The analyses were carried out at Mach number between 1.8 to 2.2 and spike angles of 12 and 20°. The flow field was subdivided into external part which was solved analytically and internal part which was solved numerically. The numerical analyses ware carried out under two assumptions; method I: non viscous flow and method II: viscous flow. The results are presented and compared based on the predicted values of the pressure recovery at the face of the compressor. The procedure was verified by comparing with previous experimental works. It was found that the pressure recovery is slightly influenced by the viscosity up to 2.14 Mach. The pressure recovery values predicted from the non viscous assumption were higher than the corresponding values obtained from the viscous solution. The viscosity contribution becomes more significant as the spike angle is increased from 12 to 20° where noticeable differences in the pressure recovery values were predicted. Accordingly, the diffusion analysis of compressible flow in such conditions assuming viscous, is essential.

Key words: Aero engine compressible flow, diffuser, numerical analysis, supersonic flow, supersonic intake

INTRODUCTION

Since the early eighties, the trend towards the numerical techniques has been widely adopted to reduce time and cost effectiveness of supersonic intake analysis, compared to the experimental investigations. The computational simulation of complex flow fields as the case of spiked supersonic inlets with shock waves presence is experienced to have complexity and not solvable, in some situations. To simplify the simulation process, it is quite common to assume 2-D flow field, symmetrical geometry and non-viscous flow.

Moretti (1988) presented an effective 2-D Euler computational technique at any number of shocks of any shape and any type. Dudek *et al*. (1996) have solved numerically for the turbulent, subsonic flow in pipe attached to conical diffusing section with 5o diffusing angle. The computations were performed to set a number of iterations until the convergence histories were leveled out.

Yu *et al.* (2010) have derived fourth order partial differential equations in the form of Euler equation to develop image restoration method. The developed algorithm solved the equation by least-square and regularization. The method represents a technique to restore the restore degraded image.

Abbood (1999) carried out numerical time dependent analysis of 2-D convergent-divergent nozzle. The procedure is based on the explicit; second order accurate McCormack predictor corrector scheme. This finite difference method required an axis transformation from the physical to computational domain. Following the experimental work of Yanta *et al.* (1990) on the 2-D scramjet inlet, Gokhel and Kumar (2001) have carried out numerical analysis on the same geometry of the inlet. They have assumed viscous adiabatic flow. The analysis was carried out on 10° single deflection wedge at 2.5 Mach and 3 Mach. Their results are in good agreement with the experimental data of Yanta *et al.* (1990) and the analysis is capable to capture the shock waves and their interaction with boundary layer. Fayadh (2000) carried out the solution of the external supersonic flow of the intake using McCormack explicit method for solving viscous, 2-D, full Navier - Stokes equations. The results showed that great deal of computation time is needed to solve these problems with explicit methods. Al-Kayiem and Sahi (2007) presented analysis procedure for single deflection 2-D spiked intake flow, assuming non-viscous supersonic flow. The external region was solved analytically while the internal part of the intake which represents the diffuser flow, has been solved numerically by solving Euler equation using Newton-Raphson iterative method. The analysis was carried out for different Angles of Attack (AOA). Al-Kayiem and Sahi (2007) have solved numerically a 2-D and viscous supersonic spiked intake to investigate the pressure distribution at the compressor face. The analysis was carried out at different forebody-Incident combinations at different supersonic fly speeds ranging from 1.8 to 2.2 Mach. CFD analysis using Control Volume Formulation technique was applied to analyze the internal flow. There results have shown that as Mach number increases, the error in total pressure recovery increases.

Xingwei and Chaoying (2011) described numerical procedure to solve for the aerodynamic characteristics of flapping airfoil in plunging motion. They have solved Navier-Stokes equation under 2-D, time dependent and incompressible flow by finite element technique.

The objective of the present study is the presentation of two analysis procedures of the compressible flow field in spiked supersonic intakes. Focus is made to highlight the error that may associate due to the viscous and non viscous flow assumption in the analysis of compressible flow diffusion.

MATERIALS AND METHODS

The aero engines consist of, in basic, an inlet, compressor, combustor, gas turbine and exit nozzle. The inlet, or so called intake, consists of two main parts: the spike and the subsonic diffuser. It is essential to reduce the incoming flow velocity from supersonic to subsonic prior to inlet to the compressor stages to avoid the presence of shock waves at the first stage stators. The spike installation provides many requirements for the engine to continuously operate in smooth modes, (Goldsmith and Seddon, 1999).

When supersonic flow approaches the spike nose, a shock system is created due to the deflections of the flow as shown in Fig. 1.

Hypothesis and analysis methodology: The supersonic flow which subjected to changes as approaching the spike was subdivided into two regions, external and internal. The external region

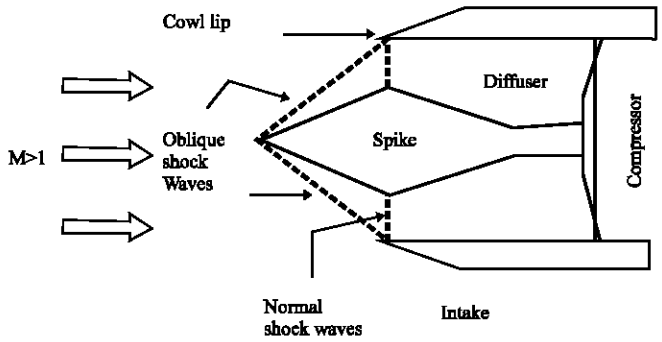

Fig. 1: Conventions of the supersonic intake

consists of the waves system created on the nose up to the normal shock wave at the smallest diffuser area. This external region is solved analytically using the set of Eq. 1 to 6. The internal region which is the subsonic compressible diffuser, is solved numerically under two different assumptions. First, is by assuming non viscous flow and second is by assuming viscous flow.

The intake model: The geometries of the 2-D supersonic spiked intake model were approximated to simulate the experimentally reported spikes by NACA (Goldsmith and Seddon, 1999). The spike has an aspect ratio, $h_{c.l}$ equals to 0.6. Conventions of the model in dimensionless format are shown in Fig. 2.

Prediction of the external flow: The region consists of the shock system is solved using the isentropic, 1-D gas dynamics relations which are available in many compressible flow texts, e.g., Anderson (2004). The flow approaches the intake at M_1. At the nose of the spike, the flow deflects with angle, δ and an OSW is created with angle, σ which could be estimated from Eq. 1, as:

$$\tan\delta = \frac{2\cot\sigma\left(M_1^2\sin^2\sigma - 1\right)}{2 + M_1^2\left(k + \cos 2\sigma\right)} \tag{1}$$

Equation 1 is solved iteratively at each free Mach, M_1 and spike angle, 2 δ. Then the Mach value behind the OSW, M_2 is evaluated from:

$$M_2 = \sqrt{\frac{(k-1)M_1^2\sin^2\sigma + 2}{2k\,M_1^2\sin^2\sigma - (k-1)}\,\frac{1}{\sin^2(\sigma-\delta)}} \tag{2}$$

And consequently, the other properties of the flow behind the OSW, including pressure p, total pressure p_o, temperature T and density ρ are predicted using Eq. 3-6.

$$\frac{P_2}{P_1} = \frac{2k}{k+1}M_1^2\sin^2\sigma - \frac{k-1}{k+1} \tag{3}$$

$$\frac{\rho_2}{\rho_1} = \frac{(k+1)M_1^2\sin^2\sigma}{2 + (k-1)M_1^2\sin^2\sigma} \tag{4}$$

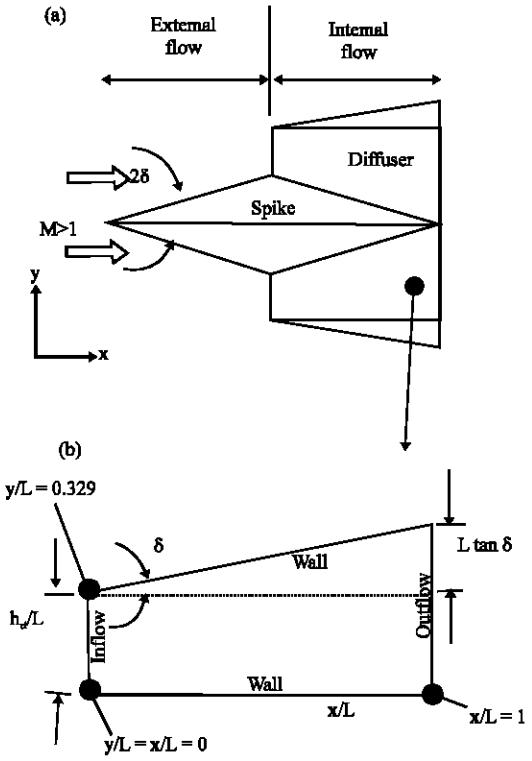

Fig. 2(a-b): The spiked intake model (a) Physical domain (b) Computational domain

$$\frac{T_2}{T_1}=\left(\frac{2k}{k+1}M_1^{\,2}\sin^2\sigma-\frac{k-1}{k+1}\right)\times\left(\frac{2+(k-1)M_1^{\,2}\sin^2\sigma}{(k+1)M_1^{\,2}\sin^2\sigma}\right) \tag{5}$$

$$\frac{Po_2}{Po_1}=\frac{P_2}{P_1}\left(\frac{1+\frac{k-1}{2}M_2^{\,2}}{1+\frac{k-1}{2}M_1^{\,2}}\right)^{\frac{k}{k-1}} \tag{6}$$

At the area between the cowl lip and the spike, a NSW is presence. The flow properties across the NSW with $M_2 = M_x$, are estimated using Eq. 7, 8 and 9:

$$M_y=\sqrt{\frac{(k-1)M_x^{\,2}+2}{2k\,M_x^{\,2}-(k-1)}} \tag{7}$$

$$\frac{P_y}{P_x}=\frac{2k}{k+1}M_x^{\,2}-\frac{k-1}{k+1} \tag{8}$$

$$\frac{Po_y}{Po_x}=\left(\frac{2k}{k+1}M_x^{\,2}-\frac{k-1}{k+1}\right)^{\frac{-1}{k-1}}\left(\frac{(k+1)M_x^{\,2}}{2+(k-1)M_x^{\,2}}\right)^{\frac{k}{k-1}} \tag{9}$$

The subscripts 1 and 2 in Eq. 1 to 6 refer to before and after the O.S.W, while subscripts x and y in Eq. 7 to 9 are referring to before and after the N.S.W.

The set of the one dimensional compressible flow Eq. 1 to 9 are converted to a computer program. The evaluated properties at station *y* are representing the boundary conditions of the inflow to the diffuser which is compressible, subsonic flow.

Prediction of the internal flow: The flow in the diffuser part of the spike is simulated numerically and solved by CFD techniques. Two simulation methods have been proposed in the present analysis under two different viscosity assumptions.

Simulation method I: Non viscous flow assumption: The governing equations of the steady, 2-D, compressible and non viscous flow are:

The continuity equation, as:

$$\left[\frac{\partial(\rho u)}{\partial x}+\frac{\partial(\rho v)}{\partial y}\right]=0 \tag{10}$$

The momentum is represented by Euler equation, in x and y directions, as:

$$\left[\frac{\partial(\rho uu)}{\partial x}+\frac{\partial(\rho uv)}{\partial y}\right]=-\frac{\partial p}{\partial x} \tag{11a}$$

$$\left[\frac{\partial(\rho vu)}{\partial x}+\frac{\partial(\rho vv)}{\partial y}\right]=-\frac{\partial p}{\partial y} \tag{11b}$$

The energy equation, as:

$$u\frac{\partial}{\partial x}\left[C_pT+\frac{\left(u^2+v^2\right)}{2}\right]+v\frac{\partial}{\partial y}\left[C_pT+\frac{\left(u^2+v^2\right)}{2}\right]=0 \tag{12}$$

where, u and v are the velocity components in x and y directions, respectively.

The state equation, after being derived with respect to x and y, as:

$$\frac{\partial p}{\partial x}=R\left[\rho\frac{\partial T}{\partial x}+T\frac{\partial \rho}{\partial x}\right] \tag{13a}$$

$$\frac{\partial p}{\partial y}=R\left[\rho\frac{\partial T}{\partial y}+T\frac{\partial \rho}{\partial y}\right] \tag{13b}$$

The diffuser is discretized to i = 1 to n segments in the axial direction and j = 1 to m segments in the transverse direction. Finite difference with axis transformation is adopted to convert the physical domain to computational domain. An in-house code is established to solve the discretized governing equations and the total pressure recovery at each operational condition is predicted.

Simulation method II: Viscous flow assumption: The mass and momentum governing equations of the steady, 2-D, compressible and viscous flow are derived from Navier-Stokes equation as:

$$\rho\frac{\partial u}{\partial x}+u\frac{\partial \rho}{\partial x}+\rho\frac{\partial v}{\partial y}+v\frac{\partial \rho}{\partial y}=0 \tag{14}$$

$$u\frac{\partial u}{\partial x}+v\frac{\partial u}{\partial y}+\frac{1}{\rho}\frac{\partial P}{\partial x}=\frac{\mu}{\rho}\left(\frac{\partial^2 u}{\partial x^2}+\frac{\partial^2 u}{\partial y^2}\right) \tag{15a}$$

$$u\frac{\partial v}{\partial x}+v\frac{\partial v}{\partial y}+\frac{1}{\rho}\frac{\partial P}{\partial y}=\frac{\mu}{\rho}\left(\frac{\partial^2 v}{\partial x^2}+\frac{\partial^2 v}{\partial y^2}\right) \tag{15b}$$

The temperature at each plane across the flow is predicted using 1-D approximation as:

$$T_{i+1} = T_i + dT \tag{16a}$$

Where:

$$dT = T\left\{-\frac{(k-1)M^2}{1+(k-1)\frac{M^2}{2}}\cdot\frac{dM}{M}\right\} \tag{16b}$$

And the Mach is predicted as:

$$M_{i+1} = M_i + dM \tag{17}$$

Where:

$$dM = M\left\{-\left[\frac{1+(\gamma-1)\frac{M^2}{2}}{1-M^2}\right]\frac{dA}{A}+\left[\frac{1+(\gamma-1)\frac{M^2}{2}}{1-M^2}\right]\frac{\gamma M^2}{2}\frac{4fdx}{D_H}\right\} \tag{18}$$

The hydraulic diameter is:

$$D_H = \frac{4\ \text{Area}}{\text{Perimeter}} = 2y \tag{19}$$

And the friction factor is:

$$f = \frac{0.0625}{\left[\log\left(\frac{5.74}{Re^{0.9}}\right)\right]^2} \tag{20a}$$

The diffuser is subdivided into m×n control volume elements and the set of the governing equations is formatted according to the finite element method of 2-D diffusion problem suggested by Versteeg and Malalasekera (2007). The set of generated equation is solved by 'Semi-Implicit Method for Pressure Linked Equation (SIMPLE)' algorithm proposed by Anderson *et al.* (1984) and using pressure corrector scheme. Another in-house code is developed to predict the flow variables; p, p_o, T, M and the velocity components, u and v.

RESULTS AND DISCUSSION

The analyses were conducted at various operational conditions as:

- The Mach number, M: 1.8, 2 and 2.2
- The spike forebody angle, 2δ: 12° and 20°
- The operation altitude, H: 10 000 m

At such altitude, the free stream temperature, T_∞ and pressure p_8 were evaluated as:

$$T_\infty = 288.16 - 0.0065H \tag{20b}$$

$$p_\infty = 101325\left(\frac{T_\infty}{288.16}\right)^{\left(\frac{0.03415H}{288.16-T_\infty}\right)} \tag{21}$$

Validation of results: The solution results of the external region were compared with the standard gas dynamic tables. The iteration technique used for the OSW angle was within 99% agreement as in Table 1.

To verify the numerical procedures, the results were compared with previously published experimental results by NACA. The variation of total pressure recovery, $p_{o\infty}/p_{o\infty}$ results obtained at different approaching Mach numbers were compared with Englert and Obery (1952) as shown in Fig. 3. The experimental results are in good agreement and support the numerical results of the present study. In both, the experimental and the numerical, the total pressure recovery was reduced slightly as Mach increases. This is because that the higher Mach reduces the OSW angle leading to weaker shock. At 1.9 Mach, the predicted results were same as that obtained from NACA Lewis 8 by 6 foot supersonic wind tunnel results. As Mach increases, a small deviation in the predicted total pressure recovery results, TPR was noticed. The maximum difference between the experimental and numerical TPR was 3.5%, at 2.1 Mach.

To verify the prediction at various spike angles, total pressure recovery data at 2 Mach was compared with the experimental results of Connor and Meyer, 1956 as shown in Fig. 4. The predicted results were in good agreement with experimental results. Both, experimental and numerical have shown the same trend of behaviour of the spike where the maximum pressure recovery was around 0.9 and is obtained at around 15° spike angle.

The internal region was solved numerically by two assumptions. The non viscous flow assumption was analyzed by solving the set of equations from 10 to 14 using in house written code. Newton-Raphson iteration technique was used after axis transformation from physical discretized domain to computational finite difference discretized domain. The viscous flow assumption of the internal region was analyzed by solving the set of equations from 15 to 20 using SIMPLE algorithm

Table 1: Comparison of the predicted OSW angles with standard gas dynamics data

Ma	Present mathematical prediction	Standard gas dynamics data	% of error
1.8	39.48	39.5	0.05
2.0	35.24	35.0	0.68

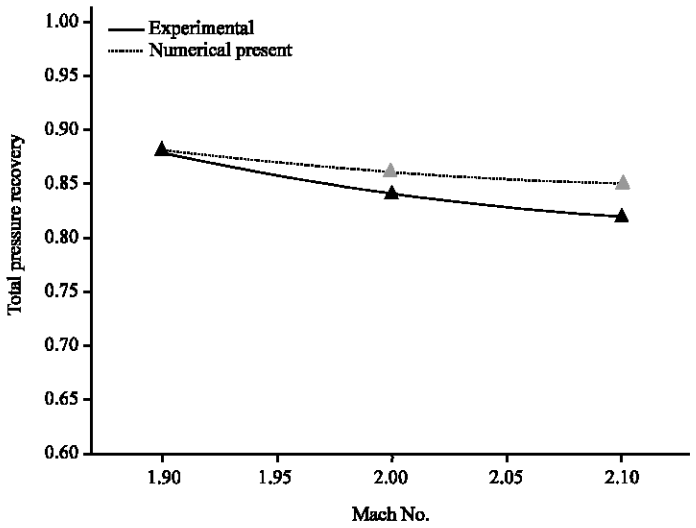

Fig. 3: Comparison with previous experimental results at various mach numbers

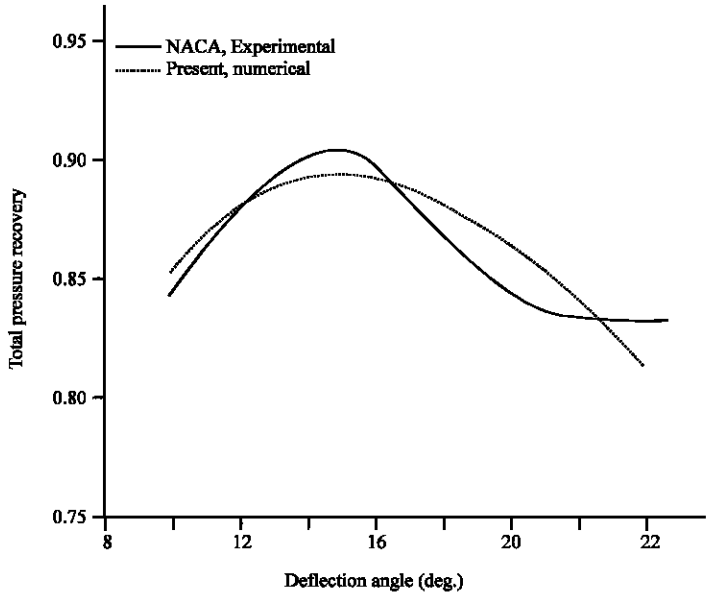

Fig. 4: Comparison with previous experimental results at various spike angles

which suggested by Patinker. The initial guess for the numerical solution was obtained by solving the 1-D, isentropic compressible flow relations.

The pressure recovery, p/p_{∞} is the dominant parameter in the analysis of the supersonic intake. It is widely used and it is an easy measured index of performance of the aero engine inlets Goldsmith and Seddon (1999).

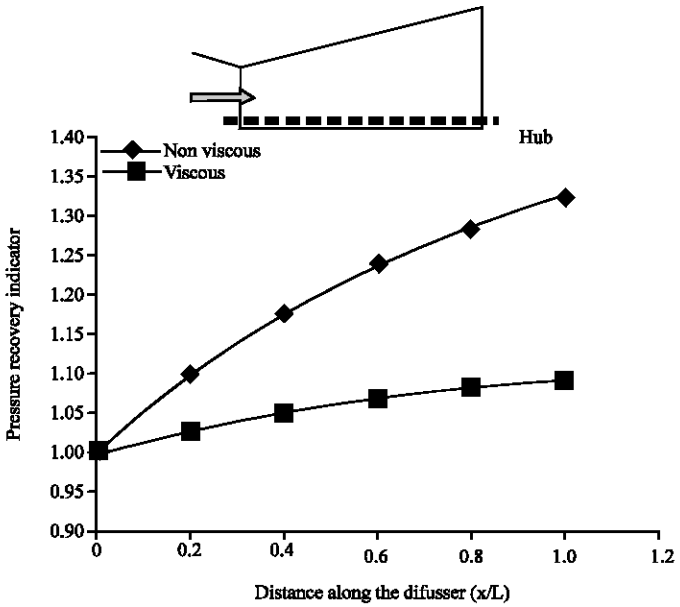

Fig. 5: Pressure results along the diffuser near the hub wall at viscous and non viscous assumptions

Viscous versus non viscous results: The first comparison between the two numerical methods were demonstrated at 2.2 Mach and the pressure recovery values have been predicted at three different locations in the diffuser along the flow path from inflow surface to outflow surface in the diffuser. Those paths were near the hub wall, in the centre of the diffuser and near the spike wall. Results of the near hub and near the spike walls were representing the predicted values in the discretization elements adjacent to the walls. The comparison reference used was the pressure recovery index which is the ratio of the pressure recovery at any location to the pressure recovery at the inlet of the diffuser which given by:

$$PRI = \frac{\left[p / p_{0\infty} \right]}{\left[p / p_{0\infty} \right]_{in}} \tag{22}$$

Figure 5 shows the results near the hub of the diffuser. The non viscous assumption leads to an overestimation in the pressure recovery. In both numerical methods, the pressure recovery increased due to the reduction in the kinetic energy of the particles in the flow which was gained by diffusion of the flow. The maximum pressure recovery was achieved at the face of the compressor. The maximum overestimation error in the PRI between the non viscous method and the viscous method was around 18%.

In the centreline of the diffuser, the same trend was observed, as shown in Fig. 6. The non viscous assumption is leading to overestimation of the pressure recovery. The maximum difference in PRI as a relative percent of error was, again, around 17%.

Figure 7 shows the results near the spike wall. The same trend of the overestimation at non viscous assumption was observed. The difference in PRI near the compressor face was 18.7% which is slightly higher than the other locations.

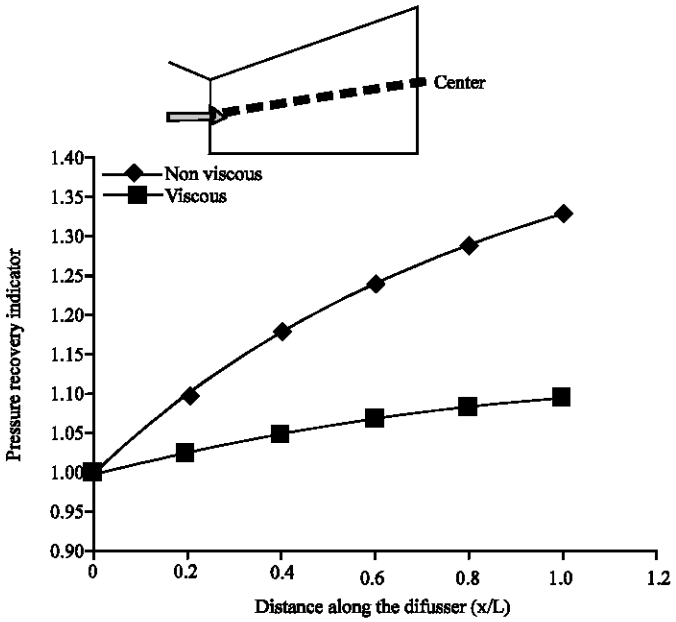

Fig. 6: Pressure results along the diffuser centre at viscous and non viscous assumptions

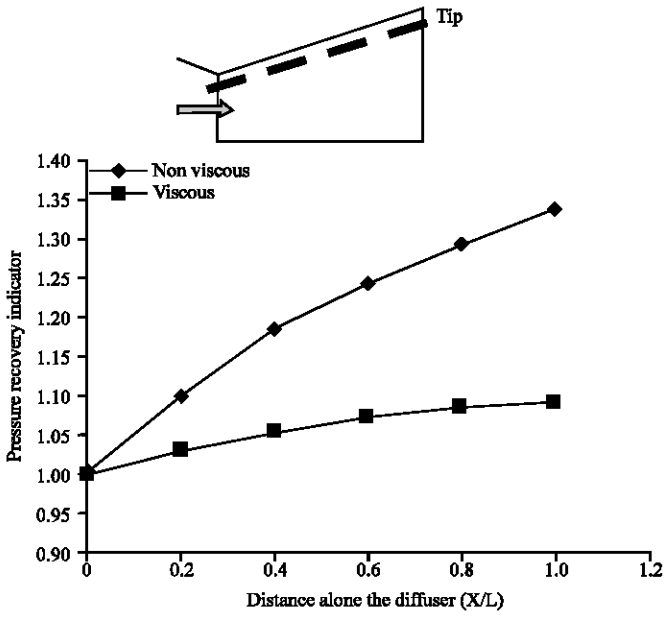

Fig. 7: Pressure results along the diffuser near the spike wall at viscous and non viscous assumptions

In general, the analysis of the results revealed that the non viscous assumption overestimated the pressure recovery near the compressor face. Similar trend of pressure recovery prediction was noticed at the tip, centre and hub. The reason behind the difference between the two numerical procedures was the presence of the boundary layer and the frictional losses in the case of the viscous flow. The non viscous could be considered as an extension to the 1-D isentropic solution where the slip conditions didn't existed. The small difference in the results between the hub and

Table 2: Comparison between viscous and non viscous results of pressure recovery at $\delta = 6°$

	Pressure recovery (PR)		
M_∞	Non viscous	Viscous	% of difference in PR
1.8	0.757	0.747	1.3
2.0	0.703	0.692	1.6
2.2	0.637	0.625	1.8

Table 3: Comparison between viscous and non viscous results of pressure recovery at $\delta = 10°$

	Pressure recovery (PR)		
M_∞	Non viscous	Viscous	% of difference in PR
1.8	0.791	0.764	3.4
2.0	0.761	0.726	4.6
2.2	0.711	0.665	6.5

the spike was due to the longer distance travelled by the air particles near the spike wall and consequently bit larger losses due to the higher shear forces on this portion of the flow.

Another comparison was carried out between the two numerical methods by comparing the pressure recovery at different free stream Mach numbers. The comparison results at different Mach with 12° spike angle and 20° are shown in Table 2 and 3, respectively. For spike angle of 12°, agreement between the two assumptions could be considered as good since the difference was very small up to Mach number 2.2 where the percentage of difference is less than 2%. For operation with higher spike angle, the non viscous assumption I not recommended. It was apparent that the viscous effects are increasingly important as the diffuser angle increases which is also demonstrated by Dudek *et al.* (1996) and Anderson (1985). The present results revealed that as the spike angle increased from 12 to 20°, the pressure recovery is enhanced but the neglect of the viscosity produced noticeable error. The non viscous assumption has shown over estimation of 3.4% at 1.8 Mach. This error increased as Mach increases reaching 6.5% when the spike angle is 20° and Mach is 2. This is due to the larger boundary layer region created near the spike wall due to the larger divergence of the flow. Hence, the non viscous assumption in the analysis of compressible diffuser flow is restricted.

CONCLUSION

The flow field within the spiked supersonic inlet of supersonic aero engine is investigated by linkage of mathematical and numerical solutions. The external part which consists of the system of the shock waves, is solved analytically by mathematical modelling. The internal part of the spike is solved numerically by two different CFD methods; firstly by assuming viscous flow and secondly non viscous flow. The numerical procedures are validated by the good agreement with previous experimental data. It could be concluded that analysis of the supersonic intake with 2-D spike is applicable with reasonable error up to 2.2 free Mach, for spike angles up to 10°. At 20° spike angle, the analysis of the flow must consider the viscosity. More spike angle is recommended to be investigated and compared with the available experimental data. Also with 10°, analyses with higher Mach values are required. The pressure recovery is enhanced as the spike angle increased from 12 to 20°. The important observation that the non viscous assumption is overestimating the pressure recovery due to the slip conditions and the neglect of the shear forces which exist in viscous flow assumption.

ACKNOWLEDGMENT

The first author acknowledges Universiti Teknologi PETRONAS for the financial and technical support to publish the study. The second author acknowledges the Commission of Military Industry-Iraq and the third author acknowledges the State of Atomic Energy-Iraq for fund granting of the research and sponsoring scholarship for their postgraduate study.

REFERENCES

Abbood, A.H., 1999. Numerical analysis of two-dimensional convergence-divergence nozzle for a modern fighter. M.Sc. Thesis, College of Military Engineering, Baghdad, Iraq.

Al-Kayiem, H.H. and A.S. Sahi, 2007. Flow analysis in spiked supersonic intakes of A/C (I-Invicid). Proceedings of AEROTECH-II, Conference on Aerospace Technology of XXI Century, June 20-21, Kuala Lumpur, Malaysia.

Anderson, D.A., J.C. Tannehill and R.H. Pletcher, 1984. Computational Fluid Mechanics and Heat Transfer. Hemisphere Publishing Corporatuion, McGraw-Hill Co., New York, USA., ISBN-13: 9780070503281, pp: 599.

Anderson, J.D., 1985. Fundamentals of Aerodynamics. McGraw-Hill Co., New York, USA..

Anderson, J.D., 2004. Modern Compressible Flow: With Historical Perspective. 3rd Edn., McGraw-Hill Co., New York, USA., ISBN-13: 978-0071121613, pp: 760.

Connor, J.F. and R.C. Meyer, 1956. Design criteria for axisymetric and two-dimensional supersonic inlets and exits. NACA-TN-3589. http://naca.central.cranfield.ac.uk/report.php?NID=6611.

Dudek, J.C., H.J. Georgiadis and D.A. Yoder, 1996. Calculation of turbulent subsonic diffuser flows using the NPARC navier-stokes code. Report No. AIAA-96-0497, National Aeronautics and Space Administration, Lewis Research Center Cleveland, Ohio, Nigeria. http://gltrs.grc.nasa.gov/cgi-bin/GLTRS/browse.pl?1996/TM-107177.html.

Englert, G.W. and L.J. Obery, 1952. Evaluation of five conical center-body supersonic diffuser at several angles of attack. NACA RM E51L04. http://aerade.cranfield.ac.uk/ara/1953/naca-rm-e53e20.pdf.

Fayadh, M.A., 2000. Numerical prediction of supersonic inviscid and viscous flows over arbitrary configurations. Ph.D. Thesis, University of Technology, Baghdad, Iraq.

Gokhel, S.S. and V.R. Kumar, 2001. Numerical computation of supersonic inlet flow. Int. J. Numer. Meth. Fluids, 36: 597-617.

Goldsmith, E.L. and J. Seddon, 1999. Intake Aerodynamic. 2nd Edn., AIAA Education Series, New York, USA., ISBN-13: 978-1563473616, pp: 407.

Moretti, G., 1988. Efficient euler solver with many applications. AIAA J., 26: 655-660.

Versteeg, H.K. and W. Malalasekera, 2007. An Introduction to Computational Fluid Dynamics: The Finite Volume Method. 2nd Edn., Pearson Education Limited, New York, USA., ISBN-13: 978-0131274983, pp: 520.

Xingwei, Z. and Z. Chaoying, 2011. Numerical investigation on the aerodynamic characteristics of a forward flight flapping airfoil with nonsymmetrical plunging motion. Inform. Technol. J., 10: 748-758.

Yanta, W.J., A.S. Collier, C. Spring, W. Boyd and J.C. McArther, 1990. Experimental measurements of the flow in scramjet inlet at mach 4. J. Propul., 6: 784-790.

Yu, X., Y. Gao, X. Yang, C. Shi and X. Yang, 2010. Image restoration method based on least-squares and regularization and fourth-order partial differential equations. Inform. Technol. J., 9: 962-967.